Controlled experiments in the earth's magnetosphere with artifical electron beams

John R. Winckler

School of Physics and Astronomy, University of Minnesota, Minneapolis, Minnesota 55455

This article describes the Electron Echo project, which used artificial electron beams to determine how natural particles are accelerated and lost from the trapping region in the earth's magnetosphere. The problems of injecting electron beams into the ionosphere, including vehicle charging and beam-plasma instabilities, are discussed, and images of the Echo beams both in space and in the laboratory are shown. The beam pulses were detected and analyzed after reflection from the conjugate hemisphere mirror points. Although the injected beams contained a wide spread of energies, the echoes displayed a monoenergetic peak, which together with the exact drift displacement during one bounce permitted a separate evaluation of electric and magnetic components of the transverse drifts in the distant magnetosphere. Thus distant electric fields were measured and found to have large turbulent fluctuations compared to the local ionospheric fields, and to differ in average value from the local fields by about 50 mV/m, indicating the existence of parallel potential drops. The measured bounce times and field-line lengths were compared with model magnetic geometries. The best fit was with the Tsyganenko-Usmanov 1982 version. Pitch-angle diffusion out of the loss cone resulted in a large loss in beam intensity during one bounce, showing the presence of important beam perturbations near the electron gyrofrequency range. Thus the Echo experiments evaluated many effects on the natural trapped particles, but were limited to a moderately disturbed condition of the magnetosphere when the magnetic morphology was stable.

CONTENTS

I. INTRODUCTION

This colloquium will describe experiments in which artificial electron beams were injected into the high-latitude ionosphere from large sounding rockets to probe plasma processes in the distant magnetosphere. These "active" experiments were motivated by the desire to obtain explicit, detailed understanding of how the Van Allen trapped radiation came to be, and were to be carried out in an active or controlled manner in the tradition of laboratory physics, so that cause and effect could be related. It was realized also that the interaction of the artificial beams with the local ionospheric plasma was a subject of great interest to the laboratory and space plasma physics community, and could be investigated while the beams were being utilized as distant probes. These "beam-plasma" studies are properly the subject of a separate paper.

Historically, active experiments on the trapped radiation were conducted on a grand scale only a few months after the discovery of the natural particles was announced by James Van Allen at a joint meeting of the American Physical Society and the National Academy of Sciences, in April 1958 in Washington D.C. (Van Allen *et al.*, 1958). The discovery, using cosmic-ray counters on the first US earth satellite *Explorer 1,* came as a complete surprise, even though the ability of the earth's dipole magnetic field to create a "mirror" geometry to contain charged particles on orbits not connected to infinity was predicted theoretically, for example, on the basis of the Stormer-Alfvén theory (Alfvén, 1953; Singer, 1957). In fact, at the time of Van Allen's discovery an ambitious program, based on a proposal by N. C. Christofilos (1959) and called the "Argus" project, was already underway by the US Advanced Research Projects Agency (ARPA) to create zones of trapped fission products from kiloton-class nuclear devices exploded in the earth's ionosphere at 480 km altitude.

The three Argus detonations were carried out in August and September 1958 and created three successive global shells of particles on dipole lines crossing the magnetic equator at about 2.1 earth radii from center. Measurements of the Argus shells by Van Allen's *Explorer 4* satellite focused wide attention on the theory of the adiabatic invariants of particle motion in the dipole geometry and showed that, although the decay of the Argus artificial belts followed an inverse time relation over many days, a vigorous magnetic storm removed the remaining artificial belts completely within a few hours.

Other, completely unrelated high-altitude nuclear tests were carried out by the US over Johnston Island in the Pacific near Hawaii, including "Teak" on 1 August, 1958 at 160 km altitude (Kellogg *et al.*, 1959) and "Starfish" on 9 July 1962 at 400 km altitude. "Starfish" created an extremely-high-intensity artificial belt in the inner radiation region, which was observed to decay over a period of several years, until it disappeared into the natural background of electrons slowly diffusing inward following ma-

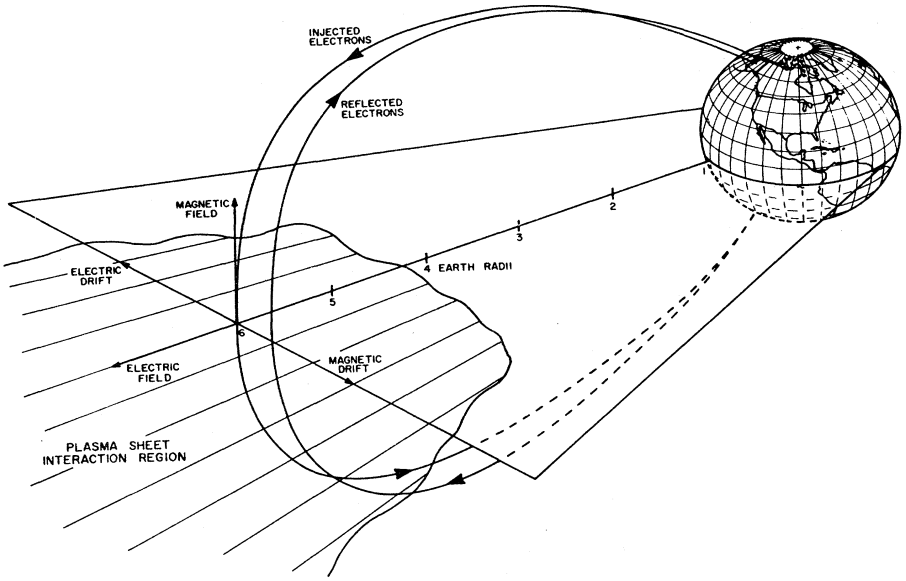

FIG. 1. Schematic of the Echo experiments. Electron beams injected from the high-latitude ionosphere are reflected from the southern-hemisphere conjugate point after possible interactions near the equatorial plane and are analyzed on return as magnetospheric probes.

jor solar activity (Pfitzer and Winckler, 1968). Both the Argus and Starfish events have been the subjects of major symposia (Christofilos, 1959; Colloq. Papers, 1963).[1]

Our present knowledge of the earth's trapped radiation may be summarized as follows: It occurs in two wide regions, a stable "inner belt" extending to about two earth radii (abbreviated RE and measured from earth center), where the particle lifetimes are surprisingly long, one year or more for electrons, and the energies high, up to 10 MeV for electrons; and an outer belt extending from 3 RE to more than 8 RE, with energies from the keV range up to 1 MeV. The particle population consists of electrons and an equal number of protons and heavier ions. The lower fringes of the trapped particles appear above 150 km altitude, well above the bulk of the neutral atmosphere, and in a region where the principal controlling force is the magnetic field B rather than collisions or gravity. More recent measurements have focused on the lower-energy magnetospheric plasmas, which have widespread consequences for magnetospheric dynamics (Kennel, 1969). The Van Allen belts may be thought of as the high-energy, suprathermal tail of this all-pervasive plasma. All solar system planets with appreciable magnetic fields are now known to have radiation belts, so that the process of injection and acceleration of the particles (if in fact there is a unique process) to MeV energies seems universal. It is certain that, although the energizing source is the solar wind plasma stream, with its entrained magnetic fields and large-scale turbulence, the energetic trapped particles do not come directly from the sun, but are accelerated locally. Both the energy-transfer mechanisms and the particle-acceleration mechanisms are known only in the form of conjectures.

After a long series of balloon, sounding rocket, and orbiting experiments, all of the "passive" type, the group at the University of Minnesota Physics Department headed by the writer decided to try to get some fundamental answers to the Van Allen belt problem by injecting coded pulsed electron beams from a high-powered rocket-borne accelerator on the same magnetic-field lines occupied by the natural particles. Although these injections were miniscule by comparison with nuclear (or natural) injections, the approach had certain advantages. For example, the beams, injected into the northern hemisphere ionosphere, could be detected after they had bounced from the southern hemisphere conjugate mirror point, so that for the first time the bounce time and corresponding field-line lengths could be measured exactly. The relatively slow "drift" motion transverse to B of the particles' centers of gyration, due to the gradient and curvature of the magnetic field and to magnetospheric electric fields, could also be measured. In addition, the scattering in pitch angle and energy changes could be studied while the beams underwent the same perturbing processes as the natural radiation belt electrons. Finally, the Echo experiments are unique in being able to identify, by the spiralling beam electrons, a known magnetic field line in space, and to compare distant Magnetospheric and nearby Ionospheric phenomena unambiguously along this line. The project was called "Electron Echo" and with

[1]See also an account of the Argus experiment by Herbert York (1987), formerly chief scientist of ARPA. See especially Chap. 7.

NASA support began with *Echo 1* in August 1970, launched on an Aerobee 350 multistage sounding rocket from the Wallops Island range in Virginia. The Echo concept is shown diagrammatically in Fig. 1. In the following 18 years, six more experiments were launched, terminating in the *Echo 7* mission in February 1988, which was the most successful of the series and the principal subject of this paper. The program through *Echo 5* has been summarized by Winckler (1982). A short summary of the "echo" aspects of the *Echo 7* experiment has recently appeared (Nemzek and Winckler, 1991a), and also a preliminary account of the entire experiment (Winckler *et al.*, 1989).

II. THE PROBLEMS OF INJECTING ELECTRON BEAMS INTO SPACE

Technically, the problem of producing intense artificial electron beams by a rocket-borne accelerator was satisfactorily solved for the purposes of the Echo series with the use of a modified Pierce-type diode (Pierce, 1949) capable of supplying up to 250 mA of current at 40 keV energy in a beam with a 2° divergence angle. The *Echo 7* 36-keV, 180-mA beam in a laboratory vacuum tank is shown in Fig. 2(b). It displays a gentle curvature in the earth's field and has a diameter of a few cm. The same beam injected into space is shown in Fig. 2(a). Here the beam is surrounded by a diffusive glow, which increases the apparent beam diameter to at least a meter, and it executes a Larmor spiral about the earth's field with a radius of 12 m. This view was recorded by a TV camera mounted on one of the three free-flying subpayloads of *Echo 7* [the plasma diagnostics payload or "PDP," as shown in the diagram in the left panel of Fig. 2(a)] as the *Echo 7* system reentered the atmosphere over Alaska near 100 km altitude, where the atmospheric density is relatively high ($6\times10^{18}/m3$). The injection pitch angle (i.e., the angle between **B** and the beam velocity **V**) was

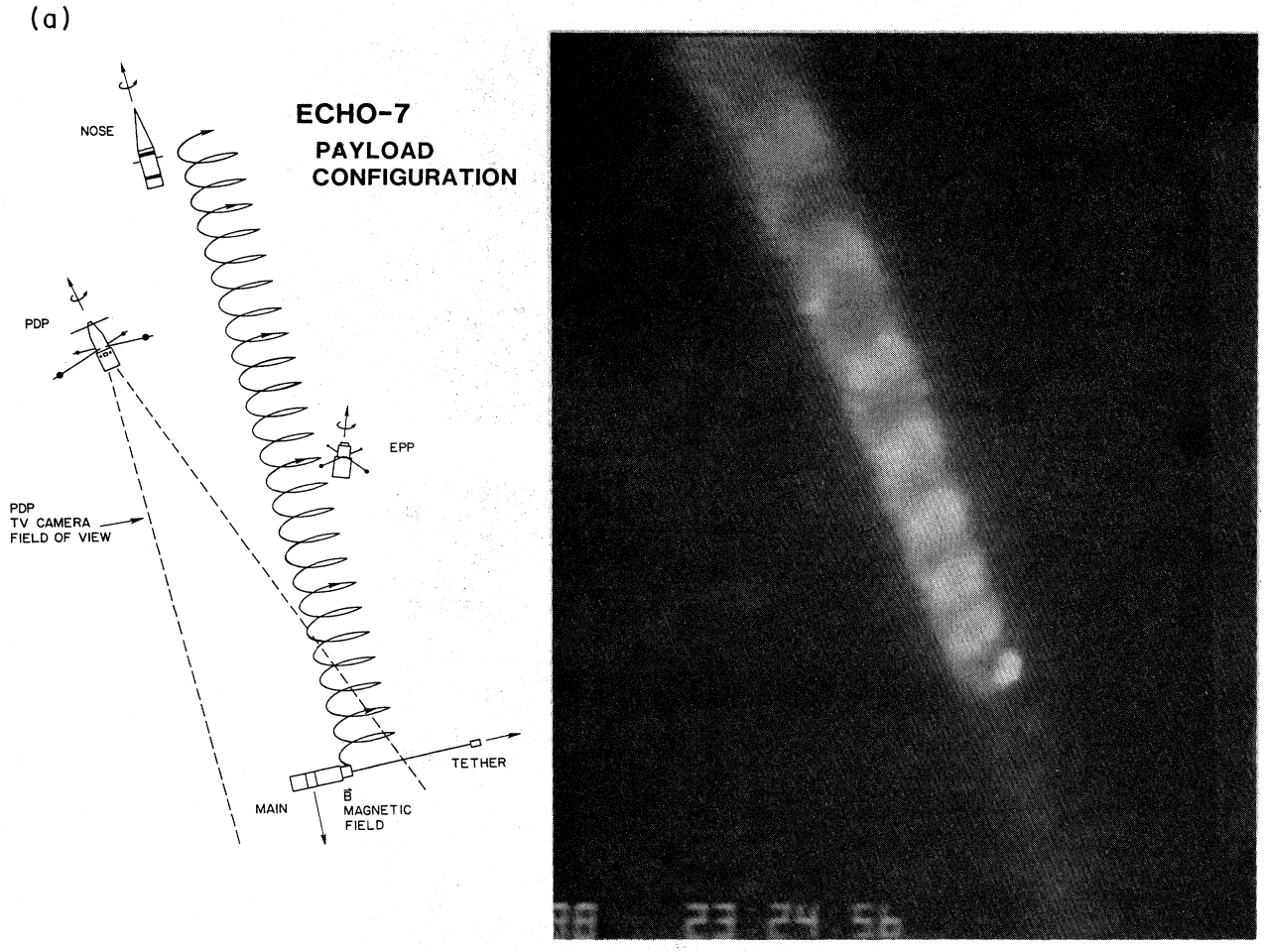

FIG. 2. Images of Echo electron beams. (a) Larmor Spiral visible near 100 km altitude (atmospheric pressure 2.4×10^{-4} Torr). The accelerator is the bright spot at bottom. (b) Beam under test in a laboratory vacuum tank (tank pressure 5×10^{-5} Torr). Note the slight curvature due to the earth's magnetic field. The accelerator is at the left. (c) Artificial auroral streak produced by beam stopping in the 90–100 km region. The accelerator was at 200 km altitude. Ground-based TV image.

120°, i.e., 30° upwards from perpendicular. At higher altitudes, near 150 km, the primary beam spiral was not visible, but instead the beam path was shown by a magnetically oriented luminous column (Fig. 3). Above 250 km the beam was not visible.

Another view of an Echo beam is shown in Fig. 2(c), recorded by a ground-based telescopic low-light-level TV system at the launch site (Poker Flat Range near Fairbanks). This artificial auroral streak extends from about 90 to 100 km and is aligned along the magnetic field. The 40-keV, 0.8-A electron beam was released from the *Echo 4* payload near 200 km altitude, was aimed downward by a programmed deflection magnet, and was stopped by atmospheric absorption, producing the observed luminosity in a narrow region around 100 km, i.e., the same region where the beam Larmor spiral in Fig. 2(b) was revealed on leaving the *Echo 7* accelerator. Such downward injections served as "marker" pulses; it was our hope that echo streaks from the conjugate region due to upward injections could also be observed by the TV on neighboring field lines. This was actually accomplished in one case (Hallinan *et al.*, 1990).

These beam images, particularly Fig. 2(c), reveal a crucial fact—that most of the beam electrons successfully escaped to infinity from the neighborhood of the accelerator vehicle. Prior to *Echo 1* in 1970, and its predecessor in space, the Hess artificial auroral rocket experiment in 1969 (Hess *et al.*, 1971), there was some doubt

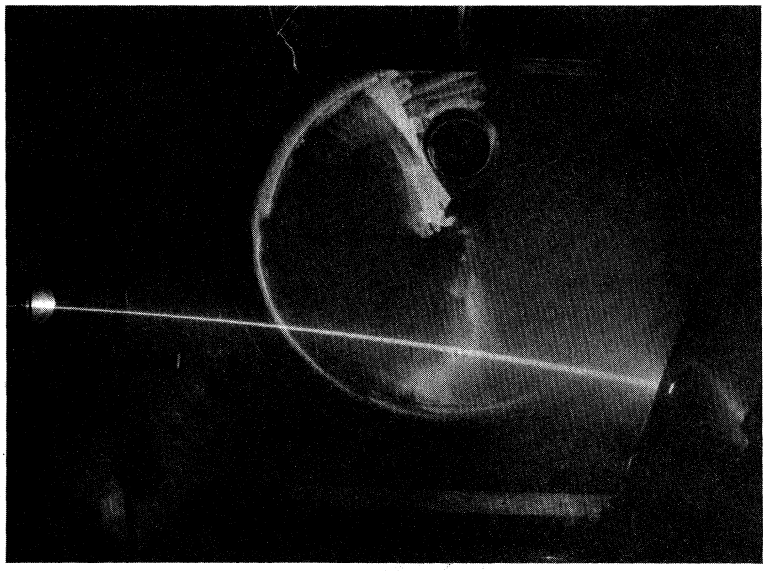

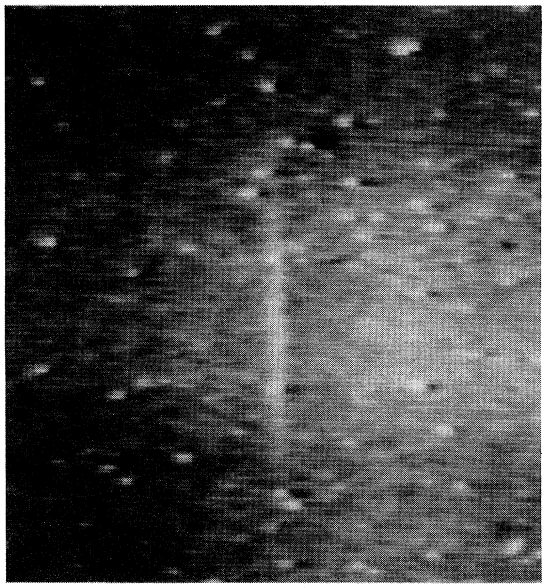

FIG. 2. (*Continued*).

that such experiments could succeed. It was feared that either the vehicle, charging to high potential, would trap the beam or that the famous two-stream instability (Bohm and Gross, 1949) would quickly thermalize the beam and prevent it from propagating coherently to large distances. That this latter process did not prove catastrophic is probably due to the small lateral dimensions of practical beams, which are not large enough compared to the wavelength of the Langmuir waves produced in the instability to trap them and permit the instability to grow to saturation (Jones and Kellogg, 1973). Nevertheless, plasma heating due to the escape of these waves from the beam is probably the cause of the extensive hot plasma region surrounding beams injected into the ionosphere. In addition, the associated strong, fluctuating electric fields in the MHz range (near the local plasma frequency) can give rise to the "beam plasma discharge" observed in laboratory tanks and in space (Getty and Smullen, 1963; Bernstein *et al.*, 1979).

The question of space vehicle charging due to beam emission or other causes has been widely discussed for several decades (Linson, 1982). Consider the following brief summary derived from Echo results: In vacuum, a rocket body of one meter radius, which has a capacity of roughly 100 pF, would charge at the rate $dV/dT = 2\times10^9$ V/s for a typical Echo beam current of 0.2 A, and would thus choke off a 40-keV beam in 20 microseconds. By contrast, the earlier Echo accelerator payloads were estimated to have charged to only several hundred volts at altitudes below 200 km. It must be remembered that the atmosphere at such heights, although called the "ionosphere," is still largely neutral. When the electron gun was started, there was a very short ($<$ ms range) transient burst of intense luminosity, followed by a continuous luminous discharge around the payload, which provided a return current from the ionosphere to the payload skin equal to the beam current. It is believed that, in such a discharge, collisionless plasma processes acted to energize secondary electrons above the 19 eV needed to ionize neutral N_2 (Galeev *et al.*, 1976). The nearby beam-generated ionization also contributed to the neutralizing current. At altitudes between 250 and 300 km, however, the *Echo 7* rocket, which was specially equipped with a small conducting tether connected to the payload by an insulated wire, showed payload charging in excess of 5 kV, and only very weak luminosity nearby.

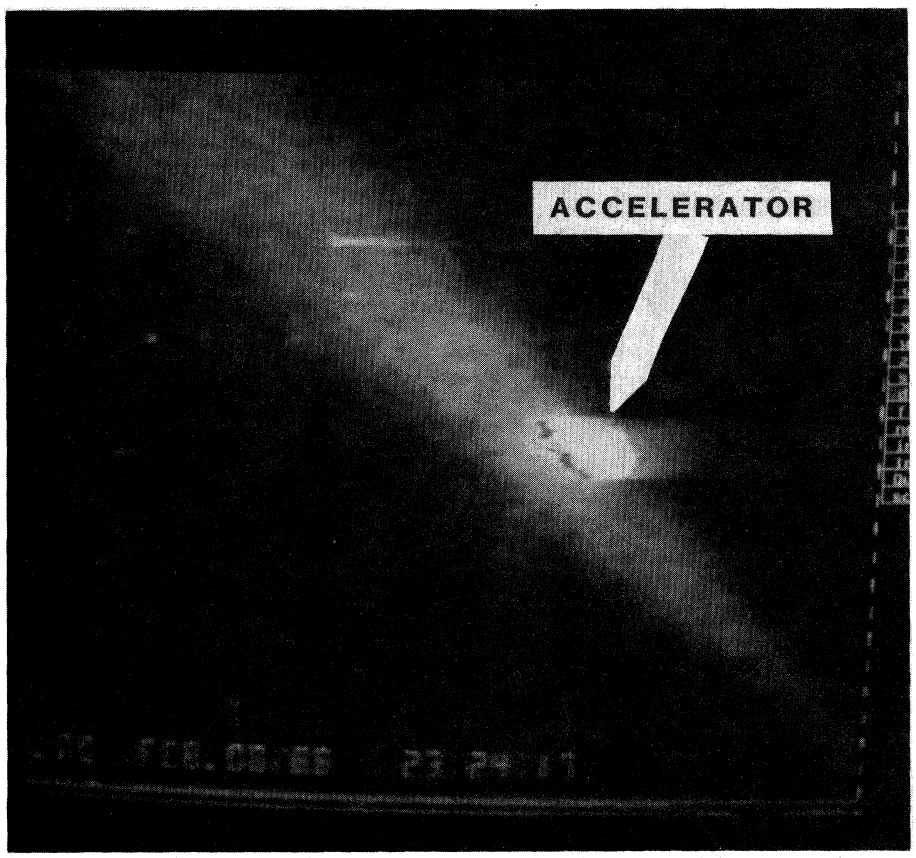

FIG. 3. The *Echo 7* beam near 150 km altitude (atmospheric pressure 4.2×10^{-6} Torr). Here the Larmor spiral is not visible, but a field-aligned column of luminosity extending up and down the field lines from the accelerator (near center) appears instead, due to secondaries. The horizontal pattern extending to the right is an artifact of the TV camera, due to overexposure in the bright glow around the accelerator.

Then, when the attitude-control-system nitrogen gas jets were fired, the emerging gas became luminous (in the shape of a butterfly, see Fig. 4), and the payload potential immediately dropped to only several hundred volts. It was also noted that most of the return current flowed through this neutral-gas luminous discharge region back to the payload skin near the jet orifices, confirming the importance of the neutral-gas environment in preventing excessive excursions of vehicle potential.

A high-altitude rocket named "*Georgia 60 Spurt,*" in honor of the 60th anniversary of the admission of the state of Georgia to the Soviet Union, was launched in 1987 by the Soviet Space Research Institute group to an altitude of 1500 km, where it was found that the payload potential rose to (or even above) the 20-kV beam accelerating voltage (Managadze *et al.*, 1988). Thus it is clear that beam-emitting vehicles can and will charge to high potentials if operated in the low densities of outer space. Fortunately, in the Echo series, payload charging was usually not large because of the limited altitude range and, even when appreciable compared to the accelerator voltage, did not seriously affect the interpretation of the echoes, as will be discussed below.

III. THE DETECTION AND ANALYSIS OF CONJUGATE ECHOES

A. Characteristics of conjugate echoes

When the Echo idea was first proposed in 1965 there were strong doubts raised that a system could be devised for detecting an electron-beam pulse which after injection into the northern hemisphere ionosphere bounced to the southern conjugate point and back—a distance of 10 to 30 times the earth's radius! But the first experiment—*Echo 1*—as well as *Echo 3, Echo 4,* and *Echo 7* proved successful in echo detection on the same vehicle system that generated the pulse, simply by sending the rocket on a magnetic easterly trajectory whose horizontal velocity approximately matched the net easterly motion of the beam electrons. As an example, in the *Echo 7* experiment, pulse-coded beams were injected in an altitude range of 200–300 km over Alaska (equatorial field-line value about 7 RE) at a typical pitch angle of 110° (20° up the field from perpendicular). Assuming adiabatic motion (which means in this case the constancy of the magnetic moment μ of the electrons due to their gyration

FIG. 4. Luminous pattern during electron-beam injection due to the two spin-attitude-control-system nitrogen gas jets (nominal atmospheric pressure 2.0×10^{-7} Torr). The electron beam is not visible, but a return-current discharge in the neutral-gas region produced the luminosity.

around the magnetic field, where $\mu = M_e V_t^2/2B$, with V_t the transverse velocity of the electrons and M_e the electron mass), the electrons would pass the equatorial plane at about 7 RE. They would then mirror at an altitude 300 km higher in the south over the Pacific Ocean west of Antarctica, and return about 2 km east of the starting point, moving downward at a 70° pitch angle. Thus the echoes were in the northern hemisphere "loss cone," i.e., they would intercept the atmosphere and generate an artificial auroral streak near 100 km altitude. At the longitude of Alaska, the southern mirror points are higher than those of the north, due to the earth's off-center equivalent magnetic dipole—a favorable situation for the Echo experiment, as the southern mirror points (adiabatically at least) lie well above the atmosphere.

It is instructive to map (or project) the various motions along magnetic-field lines onto a plane perpendicular to B called the injection plane, which over Alaska is tipped about 12° to the south from horizontal due to the inclination of the magnetic field. The rocket ballistic trajectory, which is closely parabolic in a vertical plane, is also parabolic when projected onto the injection plane, with an essentially constant eastward velocity component and a northward component that decreases to zero and reverses as the rocket passes "magnetic apogee," i.e., touches the most northerly magnetic line. The beam pulses begin on the rocket trajectory, but the projection of their motion onto the injection plane shows, besides the circular motion about their center of gyration, the relatively slow displacement of that center perpendicular to B, known as a "drift." The drift may be due to the space gradient and curvature of the magnetic field, eastward for electrons, and to magnetospheric electric fields, whose drift direction is variable, as well as to other causes whose effects are small. The projected drift speeds vary systematically as the beam spirals out along the field line, but if the net drift after one bounce equals the rocket drift, then the echoes may pass across the rocket system and be detected. This is expressed by the relation

$$\mathbf{V}_{\text{rocket}}(\perp B) = \langle \mathbf{V}_{\text{electric}} \rangle + \langle \mathbf{V}_{\text{magnetic}} \rangle \ . \tag{1}$$

The V's are bounce-averaged drift values, i.e., they equal the vector displacement after one bounce of the beam center of gyration divided by the bounce time. Note that Eq. (1) does not involve the bounce time explicitly. If the electric drift is zero, then the net drift will be magnetic and will be eastward, so that echoes can only be detected when the rocket motion is also eastward, i.e., at or near "magnetic apogee." This was the case for *Echo 1*, launched at low latitude, where electric drifts were negligible. For high latitudes, electric drifts may be large and variable, and the echo condition in Eq. (1) may be satisfied at many points on the rocket trajectory, as was the case for *Echo 4* and *Echo 7*. In detail, Eq. (1) may be written

$$\mathbf{V}_{\text{rocket}}(\perp B) = \left\langle \frac{\mathbf{E}\times\mathbf{B}}{B^2} \right\rangle + \left\langle \left[\frac{W\mathbf{R}_c\times\mathbf{B}}{qR_c^2B^2} \right](1+\cos^2\alpha) \right\rangle , \tag{2}$$

where $\mathbf{E}$ is the electric field, W the particle kinetic energy and q its charge, R_c the magnetic-field radius of curvature, and α the pitch angle. The first term on the right is the "$\mathbf{E}\times\mathbf{B}$" or electric plasma drift, which does not depend on the charge or energy of the plasma particles (see further discussion in Sec. III.C below). The second term on the right of Eq. (2) combines the magnetic gradient and curvature drifts. These drifts are eastward for electrons and vary linearly with the electron kinetic energy. This provides a means for greatly increasing the probability of echo detection by sweeping the beam energy rapidly during the injection of the coded pulses—for *Echo 7* from 40 keV to 8 keV each msec. The corresponding beam currents, following the $\frac{3}{2}$ power law for a space-charge-limited diode, varied from 225 to 25 mA. These "continuous-mode" pulses spread rapidly in the east-west direction due to the magnetic drift's dependence on energy. Their echoes mapped out, not a single point, but an extended locus with high energies to the east and low energies to the west. Figure 5 is an attempt to visualize a

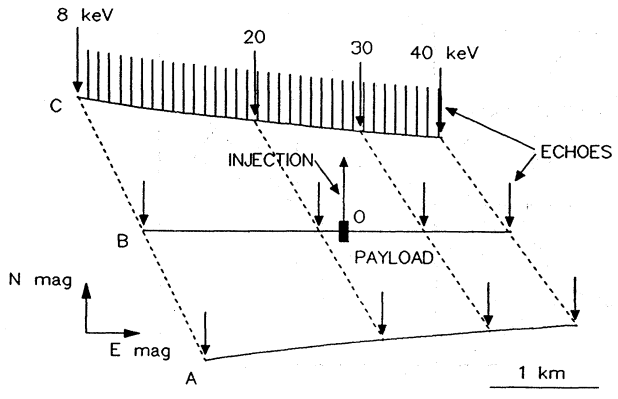

FIG. 5. Echo loci projected onto the injection plane for changing remote E-field values that bring the loci down at positions A-B-C. A monoenergetic echo is detected at O for locus B as it sweeps over the rocket.

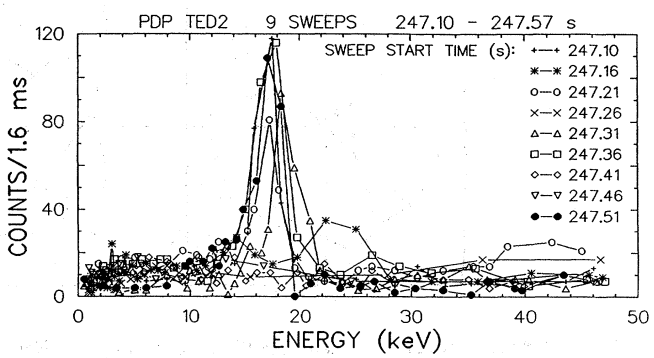

FIG. 6. Electron-energy spectrometer sweeps for a group of echoes in a 0.5-s interval. The monoenergetic peak at 18 keV repeats in most of the nine consecutive sweeps.

typical echo locus descending on the injection plane after return from the southern hemisphere. Each point on the locus should theoretically correspond to a unique energy, and the locus is curved as the bounce times along the locus depend on energy as $W^{-1/2}$ (i.e., $1/V$). An electric field whose eastward component is increasing with time, producing a northward shift of the echo locus from *A* to *B* to *C*, is assumed to exist in the distant magnetosphere. At the point "O" on *B*, the locus sweeps over the payload and is detected. Thus, although the injected beam had a wide spread of energies, the detected echo should consist of a monoenergetic peak at the energy *W* given by Eq. (2). This was demonstrated for the first time in the Echo program by *Echo 7*, as shown in Fig. 6 by the sharply peaked energy distributions for a set of echoes measured by a large-aperture electrostatic deflection electron spectrometer. The magnetosphere and the rocket system acted as a huge magnetic spectrometer, separating electrons with 18 keV energy from the continuous injection! In the case of *Echo 7* a highly variable distant electric field swept the echo locus repeatedly over the detectors, so that hundreds of echoes were observed during the flight, even at points removed from "magnetic apogee."

Another striking and unexpected feature of conjugate echoes is their compactness in a direction perpendicular to the drift shell. Figure 7, derived from the *Echo 4* experiment, demonstrates that the echo locus has a width comparable to the gyrodiameter of a single electron in the beam. Using an array of detectors whose response directions were distributed around the magnetic axis, we determined the electron intensities circulating about gyro centers in nearby space as an echo passed over the system. At *A* the echo was detected but its gyrocenter lay to the south. The echo was centered over the system at *B* and *C* and passed to the north in *D*. The polar intensity diagrams correspond to various times in the nominal echo intensity-time pulse as shown in the top panel. The electron intensity dropped off to a low value almost within a gyroradius, even though the echo was the third conjugate bounce following a single high-powered injection about nine seconds earlier. The complete history of this multiple-bounce event, in Fig. 8, shows a linear decay on a semi-log scale, which means a constant fractional loss per bounce. A similar result was obtained from a multiple-bounce event during the *Echo 7* flight (see further discussion of beam loss in Sec. III.D below).

An immediate conclusion from these echo characteristics is that *lateral* diffusive spreading of electrons was small away from the injection field line under the magnetospheric conditions of the *Echo 7* experiment. The decay in the intensity of echoes, however, indicates that major diffusion of the beams in *pitch angle* had occurred, so that the average pitch angle increased and the mirror points of the returning echoes diffused upward above the altitude of the detection system; thus part of the artificial beams joined the trapped radiation.

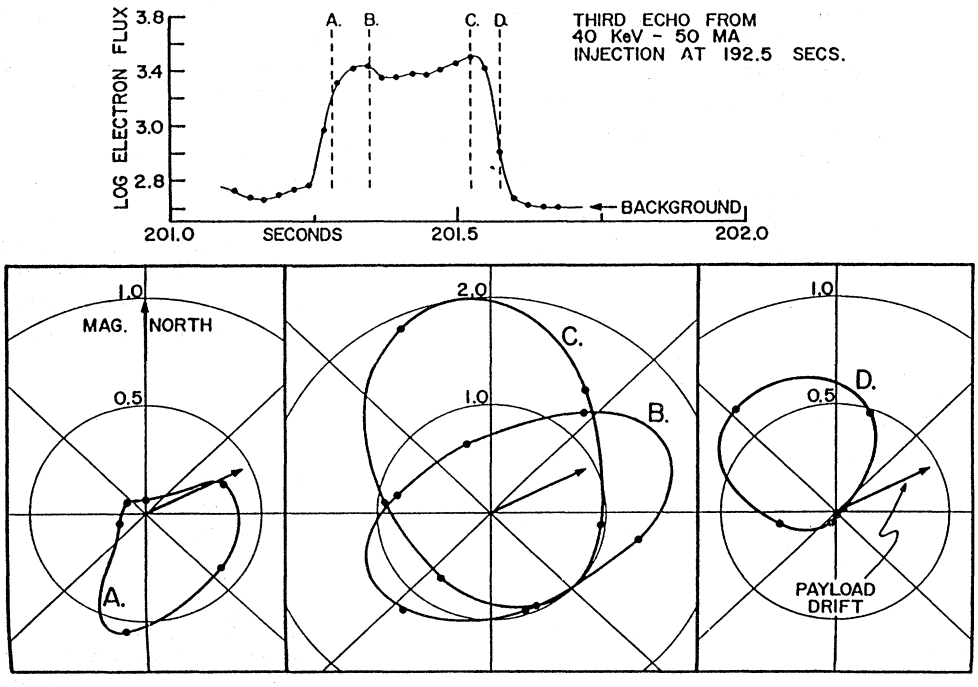

FIG. 7. (Upper) An echo intensity profile recorded by the *Echo 4* experiment, the third in a sequence of four conjugate bounces from a single injection. (Lower) Polar diagrams of flux versus direction, obtained by six scintillation detectors spaced 60° around the magnetic axis. The points give the relative flux of electrons circulating around gyrocenters one gyroradius from the rocket, in the directions shown and at the times *A-B-C-D* (upper panel).

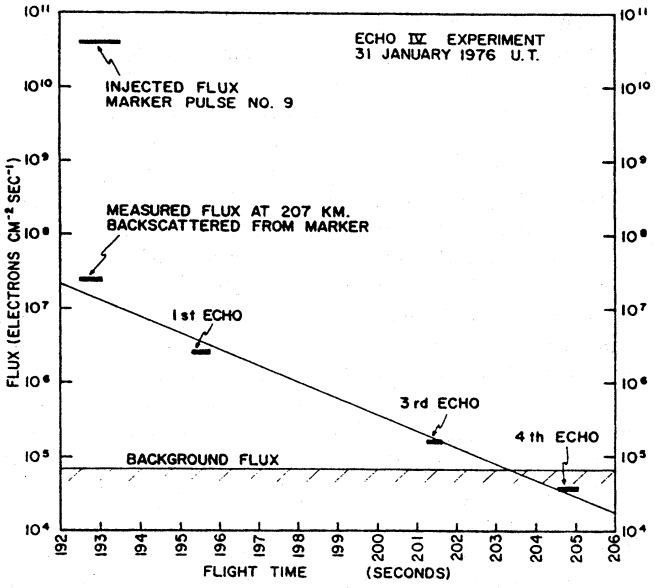

FIG. 8. A multiple-bounce conjugate echo event recorded by *Echo 4*. The event was initiated by a single downward injection, which subsequently backscattered upward to start the echo train. Note the straight-line decay on semi-log format, indicating a constant intensity loss per bounce.

B. Bounce time and field-line length measurements

Six echo groups measured during *Echo 7*'s flight had enough continuity to be matched unambiguously to the gun pulse sequence in which they originated, as demonstrated by the example in Fig. 9. The gun code (lower panel of Fig. 9) consisted of pulses of 50, 100, or 150 ms with 50-ms spaces, coded so that any train of five pulses was unique. The conjugate echo samples shown (upper panel) were recorded by two independent scintillation counters and contain responses from previous injections, as well as the echo sequence with a delay of 2.75 s from the first gun sequence shown. The echoes are shown on a log scale and are very intense compared to background. The echo intensity pattern is rounded by dispersion, and some of the pulses are not clearly resolved, but there can be no question about the identification with the gun pulse sequence. Other echoes gave bounce times between 2.4 and 3.5 s. The energy peak was measured for each echo series, and these varied in value as the varying remote electric field changed the east-west position of the locus and brought different energy regions over the detectors. However, the bounce times were found to vary proportional to $W^{-1/2}$ (i.e., to $1/V$), showing that the electrons underwent adiabatic motion through a stable magnetic field during the period. To a sufficient approximation, the magnetic-field-line length can be calculated from

$$\mathbf{S}_{\text{effective}}=\mathbf{V}_0\frac{\tau}{2}\ , \tag{3}$$

where $\mathbf{V}_0$ is the total particle velocity.

The next step in the analysis was to compare the measured field-line lengths from Eq. (3), which varied somewhat as the rocket moved to higher and then lower magnetic latitudes, with the adiabatic bounce times calculated from various model fields, with the results shown in Fig. 10. A dipole field model gave field-line lengths of approximately 95×10^3 km, much too short for agreement with observations. On the other hand, the field lines of the Olson-Pfitzer dynamic model (Olson and Pfitzer, 1982) were too tail-like, giving lengths near 185×10^3 km. Although the Olson-Pfitzer 1977 quiet-time model (OP-77I) (Olson and Pfitzer, 1977) is scarcely outside the er-

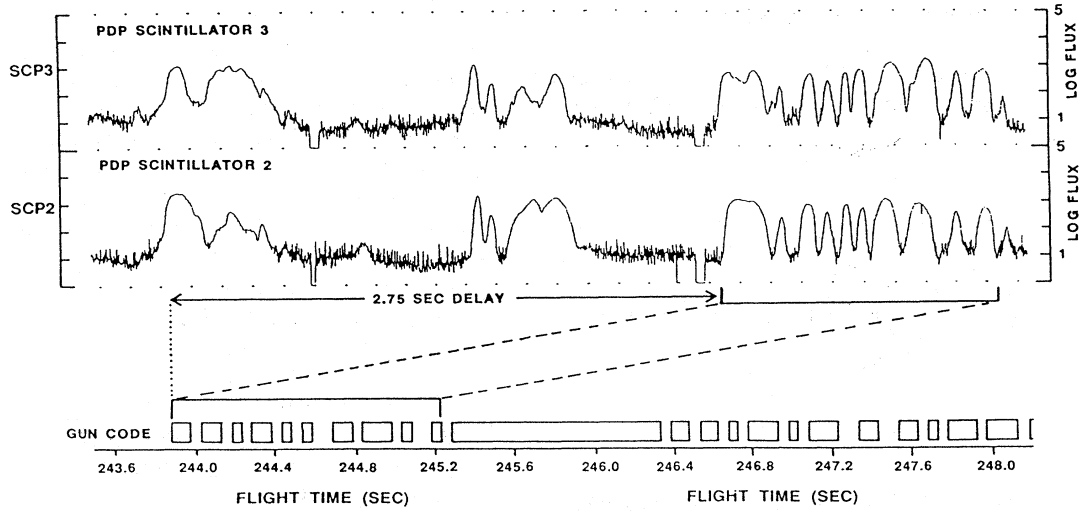

FIG. 9. An echo bounce-time measurement from *Echo 7*. The echo intensity profiles reproduce the indicated section of injected accelerator pulses. The "flight time" along the x axis refers to the rocket flight time measured from liftoff in seconds.

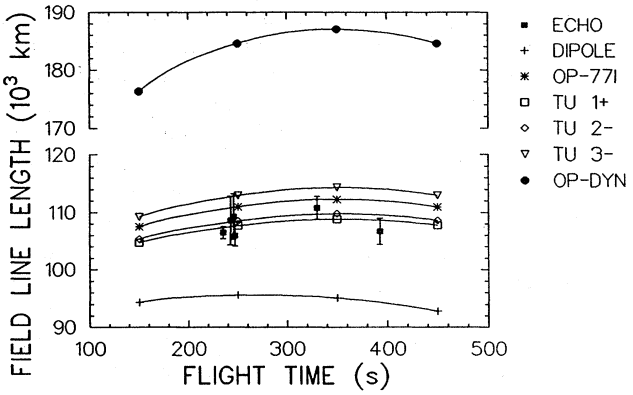

FIG. 10. Effective field-line lengths calculated from measured echoes and magnetic models.

rors, the best fit is the Tsyganenko-Usmanov (TU) model (Tsyganenko and Usmanov, 1982), with the magnetic activity parameter K_p set at 2−. A view of the inner magnetosphere with magnetic-field lines traced from this model is shown in Fig. 11. The diagram lies in the noon-midnight meridian plane, which is very close to the launch meridian of *Echo 7*. The experimental field line is seen to pass the equatorial plane at about 7 RE from center, which is in the outer radiation belt region. These night-side field lines are more extended than those due to a simple eccentric dipole model in a vacuum, an effect attributed to a dawn–dusk current "sheet" flowing in the tail plasma region. A more detailed discussion of models and their agreement with Echo results is given in Nemzek *et al.* (1992). It is essential to have a model that closely represents the actual field profile of the experiment, so that electric fields may be evaluated as described in the next section.

C. Measurement of remote electric fields

Space plasmas have a very high conductivity and basically will not support a static electric field. If, however,

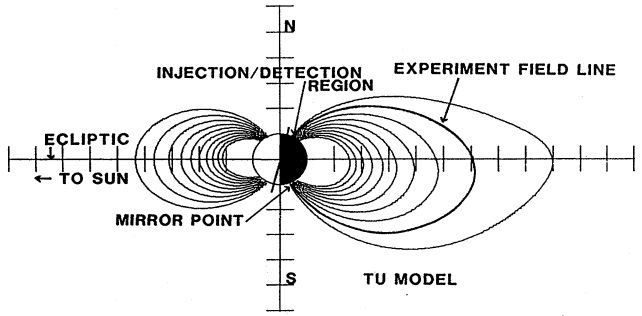

FIG. 11. The magnetic-field configuration of the inner magnetosphere as predicted by the Tsyganenko-Usmanov (TU) field model, with the magnetic activity parameter set at $Kp = 3-$, which best fit the field-line lengths derived by *Echo 7*.

the plasma is immersed in a magnetic field, as in the magnetosphere, then the plasma and magnetic force lines become "frozen" together. In the rest frame of such a plasma in space the electric field will generally again be zero, but in another inertial frame moving with respect to the magnetic field and plasma, an electric field will be measured. Thus the large-scale magnetospheric convective motions driven by the solar wind plasma stream appear in the earth reference frame as systematic patterns of electric fields (see review by Stern, 1977).

It was realized early in the Echo program that without "favorable" electric-field conditions echo observations might be difficult. But if the first term on the right side of Eq. (1) or (2) was negative (i.e., a northward electric field), this would have the effect of compensating for all or part of the magnetic drift, depending on the energy W. This made it possible for the rocket to match the net eastward electron drift without exceeding the limits on horizontal velocity imposed by the rocket range (i.e., a rocket launched from the Poker Flat range north of Fairbanks was not supposed to cross the Canadian border to the east!). Thus Echo launches were scheduled in the pre-midnight sector, when the electric field was generally northward, but this was checked by measuring the local ionospheric $\mathbf{E}\times\mathbf{B}$ drifts using an incoherent scatter radar, or by observing the ground magnetic effects of the ionospheric electric current systems (electrojets) caused by these drifts. A "northward" field here refers to the ionospheric level. Mapped into the equatorial plane, this would correspond to a radially outward field, as shown in Fig. 1. The measurement of these remote electric fields is of great interest for every phase of magnetospheric dynamics.

Evaluation of the magnetospheric electric fields from echo measurements proceeded as follows: Using the TU magnetic-field model, we evaluated the gradient-curvature term in Eq. (2) for the *Echo 7* experiment and mapped the bounce-integrated magnetic drift onto the injection plane. As the rocket drift was known, Eq. (2) could be solved for the bounce-integrated electric-field drift $\langle \mathbf{E}\times\mathbf{B}/\mathbf{B}^2 \rangle$ also evaluated at the rocket in the ionosphere. The transverse electric effect on the beam during one bounce was thus isolated and was the quantity directly measured by the experiment. The next step was to unfold $\mathbf{E}_{\text{echo}}$ from the cross product by using the known ionospheric values of B and to compare the result with *in situ* values of $\mathbf{E}$ (i.e., $\mathbf{E}_{\text{ionos}}$) measured by the electric probes on the rocket payloads, in the ionosphere at the echo detection point. This was carried out for many echoes measured by the *Echo 7* payloads, with the results shown in Fig. 12(a) for the east and Fig. 12(b) for the north electric-field components. $\mathbf{E}_{\text{ionos}}$ values lay in the range 0–30 mV/m (east) and 40–70 mV/m (north), with the variations in the 1-min time range. $\mathbf{E}_{\text{echo}}$ values were of course limited to times when echoes were detected. If Eq. (1) is split into its north and east components, it is necessary to meet the echo condition for each component separately. Thus, for the east $\mathbf{E}_{\text{echo}}$ component, values

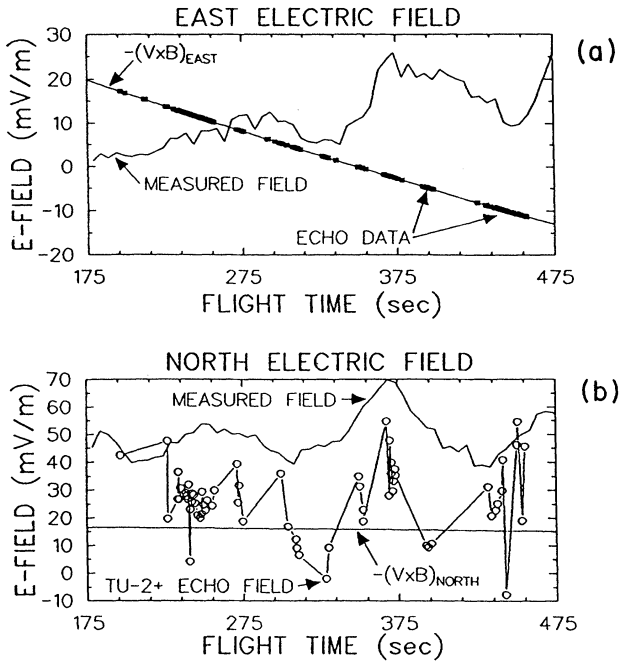

FIG. 12. Comparison of electric-field components derived from echo measurements and ionospheric measurements: (a), eastward electric-field components; (b), northward electric-field components.

were obtained only when the northward $\mathbf{E}\times\mathbf{B}$ drift matched the linearly decreasing north component of rocket motion or its electric-field equivalent, $-(\mathbf{V}\times\mathbf{B})_{east}$ (where $\mathbf{V}$ is the rocket velocity). This condition is shown by the straight line with negative slope in Fig. 12(a). The observed points lie on this line as shown. Although $\mathbf{E}_{echo}$ could be observed only along this line, it is nevertheless clear that there were large differences between the two measurements. $\mathbf{E}_{echo}$ showed much more variability than $\mathbf{E}_{ionos}$, with fluctuations extending down in time scale at least to the bounce time of several seconds.

The north electric-field component produced a westerly drift. To evaluate this component (Eq. 2), we subtracted from the rocket drift the magnetic drift calculated from the model; now, however, values were not limited by the rocket drift, because of the energy dependence of the eastward magnetic drift and the wide spread of energies injected in the beam pulses. The $\mathbf{E}_{echo}$ north field tended to reproduce the variations shown by $\mathbf{E}_{ionos}$ north, but was systematically as much as 50 mV/m smaller [Fig. 12(b)]. Another major difference was the spiky, turbulent nature of $\mathbf{E}_{echo}$, with large variations sometimes occurring for a single measurement, in this sense resembling the east component of $\mathbf{E}_{echo}$. Satellite measurements far out in the magnetosphere have found similar highly variable electric fields (Maynard *et al.*, 1982). They do not show up in the ionospheric measurements, probably because the fluctuations were damped out by finite conductivity (Labelle, 1985) before penetrating to ionospheric altitudes.

In discussing the differences shown by the above comparisons, let us assume for the moment that magnetic-field lines are equipotentials, a reasonable starting point because of the high plasma conductivity parallel to $\mathbf{B}$. This then gives a definite and simple variation of $\mathbf{E}$ with distance, that it decreases inversely with the spacing between adjacent field lines. In this case it has been shown by Roederer (1970) that the $\mathbf{E}\times\mathbf{B}$ drift at a given point along the magnetic-field line should be the same as the bounce-integrated drift to the conjugate region and back to that point. Thus if magnetic-field lines are equipotentials, $\mathbf{E}_{echo}$ and $\mathbf{E}_{ionos}$ should agree. Since this is not observed, one must conclude that the variation of $\mathbf{E}$ with distance is more complex than a simple inverse relationship with field-line spacing, that this transverse electric field contains appreciable spatial structure varying with distance along the lines of force, and also that potential drops parallel to the magnetic field must exist, at least for time scales below the 10-min duration of the measurements. These parallel fields probably supported a potential drop of 10–100 V. Additional information about echo-derived fields and their implications may be found in Nemzek and Winckler (1991b).

D. Pitch-angle diffusion and loss of electrons

The fraction of the injected beam that returned as a conjugate echo electron flux was estimated using either on-board electron counter data or ground-based low-light-level TV images of artificial auroral streaks (Hallinan *et al.*, 1990). Flights during very disturbed magnetospheric conditions (*Echo 5*) returned an echo current of less than 5% of the original beam current, while flights during moderately disturbed times measured echo currents of 20% (*Echo 7*) to 30% (*Echo 4*). These limited data suggest that the loss of echo electrons is controlled by distant magnetospheric conditions rather than beam-plasma interactions near the payload, where a relatively large change in pitch angle would be required to move the mirror heights. Near the equatorial plane, however, pitch-angle diffusion by fluctuating electric fields could be very effective. There the pitch angle and loss cone were very small (less than 2° to $\mathbf{B}$, as controlled by the first or magnetic-moment invariant), so a nonadiabatic increase of only a few eV in perpendicular energy at the equator would be required to move the entire beam out of the loss cone at rocket heights and into the inaccessible trapping region. This would amount to only a 12% increase in magnetic moment. This has been discussed in detail by Swanson, Steffen, and Winckler (Swanson *et al.*, 1986) with reference to the lack of observed optical echoes during the *Echo 5* experiment. The equatorial loss cone occupies only a very small fraction of the phase space available to electron trajectories, so the diffusion of Echo beams is essentially one way—into the trapping region. The trapped electrons, on the other

hand, fill all of phase space *except* the loss cone, so the same diffusion process brings these particles into the atmosphere (to form a diffuse aurora; see below).

IV. SUMMARY AND DISCUSSION

It will be understood that the Echo experiments have so far provided a small sampling of magnetospheric conditions, on a limited region of field lines in the outer part of the outer radiation belt region, and for particle orbits with low mirror points. The magnetic-field morphology and trapped-particle fluxes are known to undergo large changes in this region during magnetic storms (Parks and Winckler, 1968). During the *Echo 7* experiment, although the magnetic field was stable, a region of diffuse-type aurora had spread from the north, covering several degrees of latitude including the launch region. In-flight measurements showed that this layer of faint luminosity, lying near 110 km altitude, was due to a precipitation of electrons of 1–2 keV energy, probably originating in the magnetospheric tail plasma sheet reservoir (Winckler *et al.*, 1989). It is assumed that these electrons underwent a scattering process into the atmospheric loss cone near the equatorial plane. The *Echo 7* beam electrons must have sampled these same scattering mechanisms during their bounce motion. The *Echo 3* and *Echo 4* experiments encountered similar conditions. The *Echo 5* and *Echo 6* experiments, which did not observe echoes, were launched during much more disturbed conditions with bright auroral arcs present. Subject to the above qualifications, the Echo results may be summarized as follows:

(1) By simultaneous energy and bounce-time measurements magnetic-field-line lengths at an exactly specified location on the earth's surface were determined, thus fixing the parameters in a global model of the earth's exterior field. Tail field lines were found to be appreciably "inflated" compared to the dipole field, indicating the effect of external current systems. This field remained stable for times of the order of 10 minutes.

(2) Diffuse spreading of particles laterally to the field direction was found to be small over the span of several bounce periods.

(3) Pitch-angle diffusion probably occurring near the equatorial plane was found to be very important. The result would be a migration of the trapped population into the loss cone and precipitation into the auroral-zone atmosphere. This effect increased when the magnetosphere was more disturbed and has been directly observed.

(4) The distant magnetospheric electric field was found to have a turbulent, fluctuating component, which did not reach the ionosphere, but which displaced particle trajectories, by $\mathbf{E}\times\mathbf{B}$ drifts, many gyrodiameters, in times of the order of the bounce time of several seconds. This could lead ultimately to large drift-shell diffusion.

(5) A systematic difference was observed between the ionospheric and magnetospheric large-scale fields, indicating potential differences, measured parallel to **B**, of the order of 10–100 V, persisting for times at least of the order of 10 minutes. These potential drops could accelerate the thermal population of plasma parallel to **B** to generate field-aligned electric currents.

In conclusion, the Echo experiments have been successful in establishing many new details of the behavior of trapped electrons under conditions leading to their decay and loss. The more difficult measurements during an acceleration-injection period, when large energy changes of the injected beams might be expected, remain for future experiments.

ACKNOWLEDGMENTS

The Echo program has been supported at the School of Physics and Astronomy, University of Minnesota by the Space Physics Division of NASA Headquarters under Grant NSG 5088. The *Echo 7* mission was sponsored jointly by NASA and the Air Force Geophysics Laboratory, Bedford, Massachusetts. The author acknowledges the contributions of many individuals during the course of the program, but particularly, in the case of the *Echo 7* mission, the in-depth echo analysis of Dr. Robert Nemzek, the beam TV images by Dr. Robert Franz, and the payload engineering and support provided by Dr. Perry Malcolm.

REFERENCES

Alfvén, H., 1953, *Cosmical Electrodynamics* (Clarendon, Oxford).

Bernstein, W., H. Leinbach, P. J. Kellog, S. J. Momson, and T. Hallinan, 1979, "Further Laboratory Measurements of the Beam-Plasma Discharge," J. Geophys. Res. **84**, 7271.

Bohm, D., and E. P. Gross, 1949, "Theory of Plasma Oscillations, B. Excitation and Damping of Oscillations," Phys. Rev. **75**, 1864.

Christofilos, N. C., 1959, "The Argus Experiment," J. Geophys. Res. **64**, 869.

Coll. Papers, 1963, "Collected Papers on the Artificial Radiation Belt from the July 9, 1962, Nuclear Detonation," J. Geophys. Res. **68**(3), 1 February 1963.

Galeev, A. A., E. V. Mishin, R. Z. Sagdeef, V. D. Shapiro, and V. I. Shevchenko, 1976, "Discharge in the Region around a Rocket following Injection of Electron Beams into the Ionosphere" (in Russian), Dokl. Akad. Nauk SSSR **231**, 71.

Getty, W. D., and L. D. Smullin, 1963, "Beam-Plasma Discharge: Buildup of Oscillations," J. Appl. Phys. **34**, 3421.

Hallinan, T. J., J. Winckler, P. Malcolm, H. C. Stenbeck-Nielson, and James Baldridge, 1990, "Conjugate Echoes of Artificially Injected Electron Beams Detected Optically by Means of New Image Processing," J. Geophys. Res. **95**, 6519.

Hess, W. N., M. G. Trichel, T. N. Davis, W. C. Beggs, G. E. Kraft, E. Stassinopoulos, and E. J. R. Maier, 1971, "Artificial Auroral Experiment: Experiment and Principal Results," J. Geophys. Res. **84**, 1442.

Jones, T. W., and P. J. Kellogg, 1973, "Plasma Waves Artificially Induced in the Ionosphere," J. Geophys. Res. **78**, 2166.

Kellog, P. J., E. P. Ney, and J. R. Winckler, 1959, "Geophysical Effects Associated with High-Altitude Explosions," Nature **183**, 358.

Kennel, C. F., 1969, "Consequences of a Magnetospheric Plasma," Rev. Geophys. **7**, 379.

Labelle, J., 1985, "Mapping of Electric Field Structures from the Equatorial F Region to the Underlying E Region," J. Geophys. Res. **90**, 4341.

Linson, L. M., 1982, "Charge Neutralization as Studied Experimentally and Theoretically," in *Artificial Particle Beams in Space Plasma Studies,* NATO Advanced Study Institute No. 79, edited by B. Grandal (Plenum, N.Y.), p. 573.

Managadze, G. G., V. M. Balebanov, A. A. Burchudladze, T. I. Gaugua, N. A. Leonov, S. B. Lyakhov, A. A. Martinson, A. D. Mayorov, W. K. Riedler, M. F. Friedrich, K. M. Torkar, A. N. Kaliashvili, Z. Klos, and Z. Zbyszynski, 1988, "Potential Observation of an Electron Emitting Rocket Payload and Other Related Plasma Measurements," Planet. Space Sci. **36**, 399.

Maynard, N. C., J. P. Heppner, and T. L. Aggson, 1982, "Turbulent Electric Fields in the Nightside Magnetosphere," J. Geophys. Res. **87**, 1445.

Nemzek, R. J., P. R. Malcolm, and J. R. Winckler, 1992, "Comparison of Echo 7 Field-Line Length Measurements to Magneospheric Models," J. Geophys. Res. **97**, No. 2, in press.

Nemzek, R. J., and J. R. Winckler, 1991a, "Electron Beam Sounding Rocket Experiments for Probing the Distant Magnetosphere," Phys. Rev. Lett. **67**, 987.

Nemzek, R. J., and J. R. Winckler, 1991b, "Parallel Electric Fields Detected via Conjugate Electron Echoes during the Echo 7 Sounding Rocket Flight," J. Geophys. Res. **96**, 11, 475.

Olson, W P., and K. A. Pfitzer, 1977, "Magnetospheric Magnetic Field Modeling," McDonnell-Douglas Aeronautics Co. Annual Science Report (AFOSR Contract No. F-44620-75-C-0033, 1977).

Olson, W. P., and K. A. Pfitzer, 1982, "A Dynamic Model of the Magnetospheric Magnetic and Electric Fields for July 29, 1977," J. Geophys. Res. **87**, 5943.

Parks, G. K., and J. R. Winckler, 1968, "Acceleration of Energetic Electrons Observed at the Synchronous Altitude during Magnetospheric Substorms," J. Geophys. Res. **73**, 5786.

Pfitzer, K. A., and J. R. Winckler, 1968, "Experimental Observation of a Large Addition to the Electron Inner Radiation Belt after a Solar Flare Event," J. Geophys. Res. **73**, 5792.

Pierce, J. R., 1949, *Theory and Design of Electron Beams* (Van Nostrand, N.Y.).

Roederer, J. G., 1970, *Dynamics of Geomagnetically Trapped Radiation* (Springer, N.Y.), see pp. 142–145.

Singer, S. F., 1957, Trans. Am. Geophys. Union **38**, 135.

Stern, D. P., 1977, "Large-Scale Electric Fields in the Earth's Magnetosphere," Rev. Geophys. Space Phys. **15**, 156.

Swanson, R. L., J. E. Steffen, and J. R. Winckler, 1986, "The Effect of Strong Pitch Angle Scattering on the Use of Artificial Auroral Streaks for Echo Detection—Echo 5," Planet. Space Sci. **34**, 411.

Tsyganenko, N. A., and A. V. Usmanov, 1982, "Determination of the Magnetospheric Current System Parameters and Development of Experimental Magnetic Field Models Based on Data From the IMP and HEOS Satellites," Planet. Space Sci. **30**, 985.

Winckler, J. R., 1982, "The Use of Artificial Electron Beams as Probes of the Distant Magnetosphere," in *Artificial Particle Beams in Space Plasma Studies,* NATO Advanced Study Institute No. 79, edited by B. Grandal (Plenum, N.Y.), p. 3.

Winckler, J. R., P. R. Malcolm, R. L. Arnoldy, W. J. Burke, K. N. Erickson, J. Ernstmeyer, R. C. Francz, T. J. Hallinan, P. J. Kellogg, S. J. Monson, K. A. Lynch, G. Murphy, and R. J. Nemzek, 1989, "Echo 7, An Electron Beam Experiment in the Magnetosphere," EOS Trans. Am. Geophys. Union **70**, 657, 665.

Van Allen, J. A., G. H. Ludwig, E. C. Ray, and C. E. McIlwain, 1958, "Observation of High-Intensity Radiation by Satellites 1958 Alpha and Gamma," Jet Propulsion **28**, 588.

York, Herbert, 1987, *Making Weapons, Talking Peace* (Basic Books, New York).

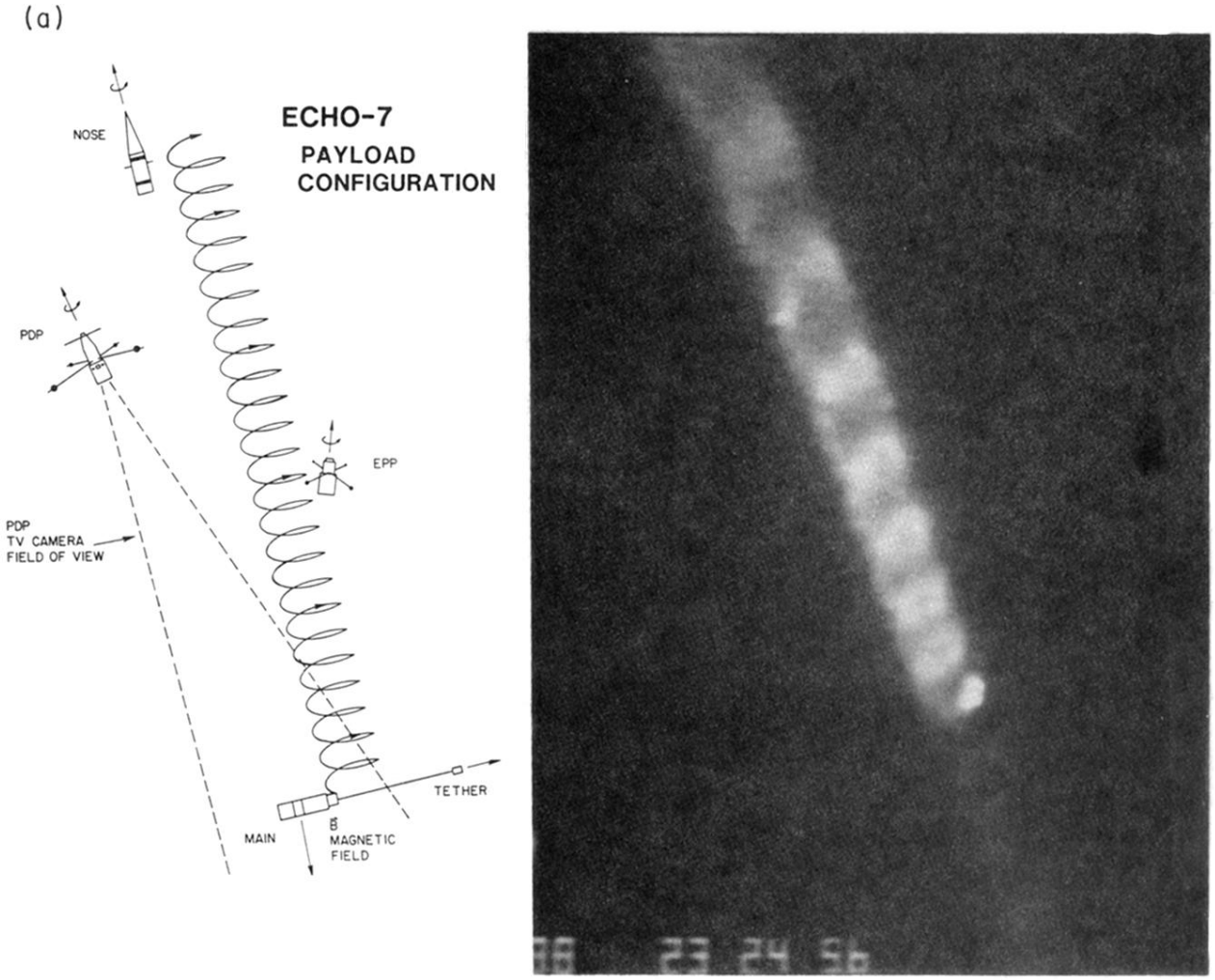

FIG. 2. Images of Echo electron beams. (a) Larmor Spiral visible near 100 km altitude (atmospheric pressure 2.4×10^{-4} Torr). The accelerator is the bright spot at bottom. (b) Beam under test in a laboratory vacuum tank (tank pressure 5×10^{-5} Torr). Note the slight curvature due to the earth's magnetic field. The accelerator is at the left. (c) Artificial auroral streak produced by beam stopping in the 90–100 km region. The accelerator was at 200 km altitude. Ground-based TV image.

(b)

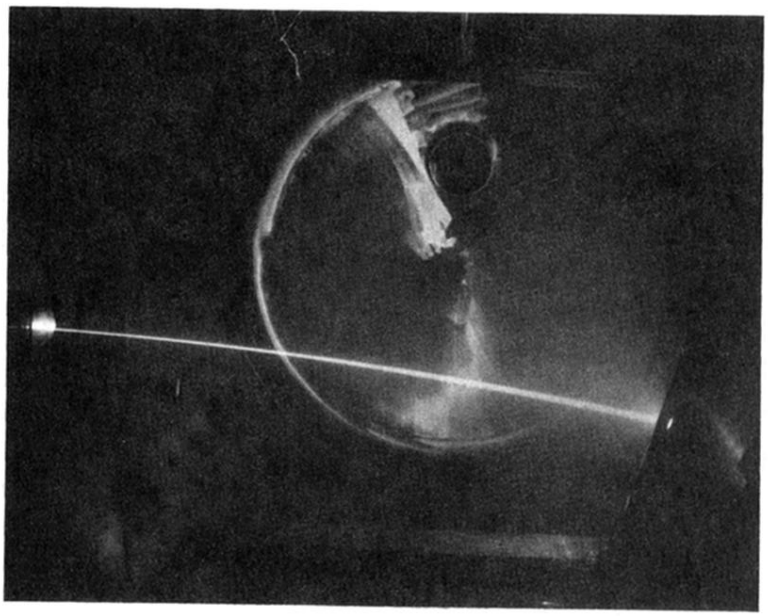

(c)

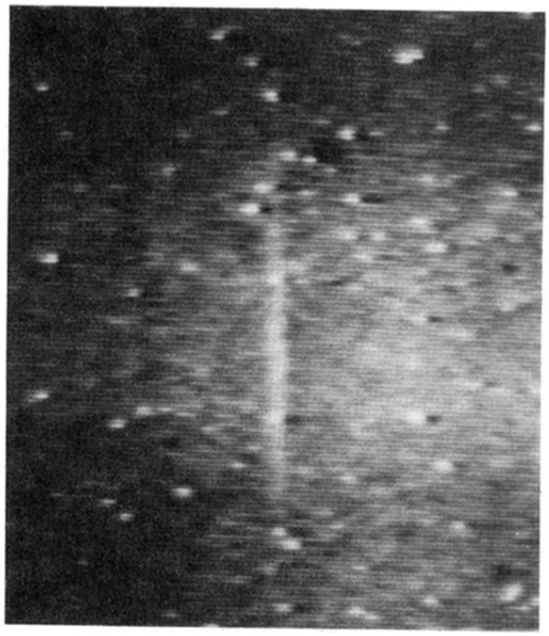

FIG. 2. (*Continued*).

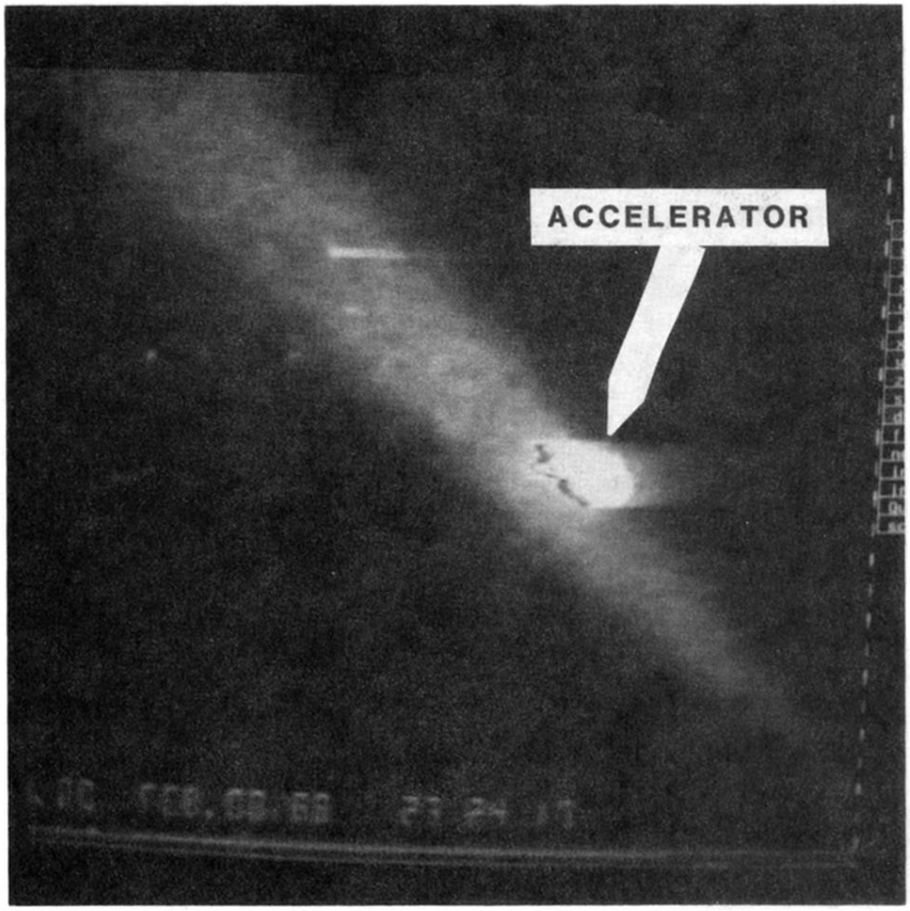

FIG. 3. The *Echo 7* beam near 150 km altitude (atmospheric pressure 4.2×10^{-6} Torr). Here the Larmor spiral is not visible, but a field-aligned column of luminosity extending up and down the field lines from the accelerator (near center) appears instead, due to secondaries. The horizontal pattern extending to the right is an artifact of the TV camera, due to overexposure in the bright glow around the accelerator.

FIG. 4. Luminous pattern during electron-beam injection due to the two spin-attitude-control-system nitrogen gas jets (nominal atmospheric pressure 2.0×10^{-7} Torr). The electron beam is not visible, but a return-current discharge in the neutral-gas region produced the luminosity.